Available online at www.sciencedirect.com

ScienceDirect

Nuclear Physics B 959 (2020) 115157

NUCLEAR PHYSICS B

www.elsevier.com/locate/nuclphysb

A comparative study of the anomalous tHq couplings via the diphoton channel at the LHC

Jie-Fen Shen *, Yan-Ju Zhang

School of Biomedical Engineering, Xinxiang Medical University, Xinxiang 453003, PR China

Received 9 June 2020; received in revised form 5 August 2020; accepted 24 August 2020
Available online 28 August 2020
Editor: Hong-Jian He

Abstract

We present a comparative study about the flavor changing neutral Higgs (FCNH) interactions of top quark, i.e., tqh ($q = u, c$), from two processes with the $h \to \gamma\gamma$ decay channel: top quark pair production $pp \to t\bar{t}$ with one top decaying to hq, and the anomalous single top plus Higgs production process $pp \to th$. We perform a full simulation for the signals and the relevant SM backgrounds based on two separate cut selections at the future 14 TeV High Luminosity LHC (HL-LHC). The results show that the SM background can be greatly reduced for both selection methods. The branching ratios of $t \to uh$ and $t \to ch$ can be, respectively, probed to 1.4×10^{-4} and 1.5×10^{-4} at the 95% Confidence Level (CL), which is consistent with the dedicated study performed by the ATLAS collaboration. The advantage of the $pp \to th$ process is that the origin of the signal from tuh or tch couplings could be clarified by studying the diphoton pseudo-rapidity and the charges of the charged lepton from the top decay. If we only consider the signal coming from this process, the upper limit on the branching ratio of about $Br(t \to uh) = 2.4 \times 10^{-4}$ at the 95% CL is obtained. Altogether, these limits are one order of magnitude better than the current 13 TeV LHC experimental results.

* Corresponding author.
E-mail address: shjf@xxmu.edu.cn (J.-F. Shen).

https://doi.org/10.1016/j.nuclphysb.2020.115157

1. Introduction

The discovery of the 125 GeV Higgs boson at the Large Hadron Collider (LHC) [1,2] opened a new era of exploring the origin of the elementary particle masses. Following that, one can expect to search new physics (NP) beyond the SM through exploring the coupling of the Higgs boson with the other elementary particles. In the SM, the flavor changing neutral Higgs (FCNH) interactions of top quark, i.e., the vertex tqh ($q = u, c$), are absent at tree-level and suppressed largely at loop-level due to the GIM mechanism [3,4]. However, the branching ratios for the $t \to qh$ decays are predicted to be in the range of $\mathcal{O}(10^{-6} - 10^{-3})$ in several extensions of the SM, e.g. supersymmetry models [5–10], two Higgs doublet models [11–15], and other NP models [16–20]. One can expect that such contribution could be discovered or constrained at the current and future LHC experiments. Thus any experimental signatures of such FCNH interactions of top quark will serve as a clear signal for NP Beyond the SM [21–23].

In general, the effective FCNH interaction between the Higgs boson and the top quark, tqh, which can be expressed as

$$\mathcal{L} = \kappa_{tuh}\bar{t}Hu + \kappa_{tch}\bar{t}Hc + h.c., \tag{1}$$

where κ_{tuh} and κ_{tch} denote the flavor changing coupling constants. Recently, the constraint on the thq interactions through direct measurements was reported by the CMS and ATLAS collaborations at $\sqrt{s} = 13$ TeV [24–27] by searching for $t\bar{t}$ production with one top decaying to Wb and the other assumed to decay to hq. For example, the combination of these searches with ATLAS searches in $h \to b\bar{b}, \tau^+\tau^-, \gamma\gamma$ and multilepton final states yields observed limits for $Br(t \to qH)$ at 95% Confidence Level (CL) [26]:

$$Br(t \to uh) \leq 1.2 \times 10^{-3}, \quad Br(t \to ch) \leq 1.1 \times 10^{-3}. \tag{2}$$

From a phenomenological viewpoint, the FCNH interactions between the Higgs boson and the top quark have been studied extensively at LHC via different processes using model-independent methods [28–34].

From previous studies we know that the FCNH interaction tqh could be probed at the LHC by two channels: the top quark pair production process $pp \to t\bar{t}$ with the anomalous decay from one top quark $t \to qh$, and the single top plus Higgs process $pp \to th$ via the anomalous tqh couplings, as shown in Fig. 1. The former process can give stronger constrains on the FCNC tqh couplings due to its larger production rate, but the latter is more sensitive to the tuh coupling and has large charge ratio for the final states [31]. Besides, the advantage of this search with respect to other searches is an explicit reconstruction of the Higgs boson which would be very useful in the case of a positive signal [32]. Because these two processes with different production mechanisms have similar final states, one needs to know which channel has the higher significance and compare their respective advantages for an inclusive search. In this paper, we perform an comparative study of FCNH interaction between the Higgs boson and the top quark at the High Luminosity (HL-LHC) run of the 14 TeV CERN collider, by considering the Higgs diphoton decay channel due to the relatively clean SM backgrounds.

This paper is arranged as follows. In Sec. 2, we perform a complete calculation of two top-higgs associated production processes by considering the FCNH interactions tqh at tree level. Besides, we discuss the observability for two dominant processes by the diphoton final state at the HL-LHC. Finally, our conclusions are presented in Sec. 3.

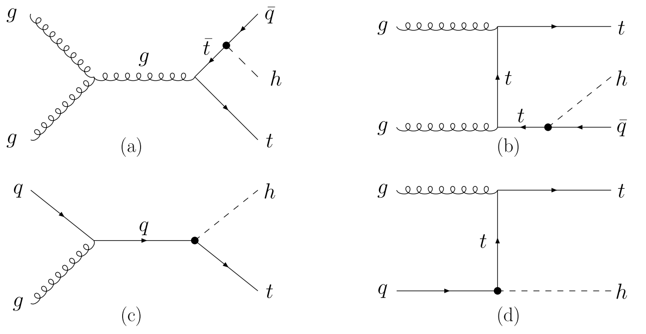

Fig. 1. Representative Feynman diagrams for: the top pair production processes $gg \to t\bar{t}$ with $\bar{t} \to \bar{q}h$ decay channel (a-b), and the top-Higgs associated production processes $qg \to th$ (c-d). Here $q = u, c$.

2. Process analysis and numerical result

2.1. Monte Carlo simulations and cuts selections

In the following we will perform the Monte Carlo simulations and look for the suitable cuts through the processes

$$pp \to t(\to W^+b \to \ell^+\nu b)h(\to \gamma\gamma), \tag{3}$$

$$pp \to t\bar{t} \to t(\to W^+b \to \ell^+\nu b)h(\to \gamma\gamma)j, \tag{4}$$

where $\ell = e, \mu$. Note that the analysis also considers the charge-conjugate process. The final state of signal process is thus characterised by two photons, exactly one lepton and one b-jet. The main SM backgrounds include the resonant backgrounds and the nonresonant backgrounds, such as $t\bar{t}h$, thj, $t\bar{t}\gamma\gamma$, $tj\gamma\gamma$ and $\gamma\gamma W^\pm jj$.

The production cross sections for the signals are calculated at the leading order (LO) by using MadGraph5-aMC@NLO [35] with NNPDF23L01 PDFs [36], considering the renormalisation and factorisation scales to be $\mu_R = \mu_F = \mu_0/2 = (m_t + m_h)/2$. In our numerical calculations, the SM input parameters are taken from Ref. [37]. The coupling parameter should satisfy the direct constraint from the current ATLAS result and is taken as $\kappa_{tqh} \leq 0.04$ [38]. All the generated parton level events are passed through PYTHIA8.20 [39] and DELPHES3.4.2 [40] for parton shower and detector simulations. Finally, event analysis is performed by using MadAnalysis5 [41]. When generating the parton level events, we assume $\mu_R = \mu_F$ to be the default event-by-event value. The anti-k_t algorithm [42] with distance parameter $R = 0.4$ is used for jet reconstruction.

Here it should be mentioned that we rescale the leading order cross sections to the corresponding NLO QCD results with the K-factor, i.e., $K = 1.5$ for the $pp \to th$ process [43] and $K = 1.18$ for the $pp \to t\bar{t}h$ process [44]. The dominant $t\bar{t}$ produced process is normalized to the NNLO total cross section as studied in [45]. For other SM background processes, we have rescaled their cross sections by a K-factor of 1.5. This approximation does not have a significant impact on our derived sensitivities.

In order to identify objects, we chose the basic cuts at parton level for the signals and SM backgrounds as follows:

$$\begin{aligned} &\Delta R_{ij} > 0.4\,, \quad i,j = \gamma, \ell, b \text{ or } j \\ &p_T^{\gamma,\ell} > 20\text{ GeV}, \quad |\eta_{\gamma,\ell}| < 2.5 \\ &p_T^{b} > 25\text{ GeV}, \quad |\eta_{b}| < 2.5 \\ &p_T^{j} > 25\text{ GeV}, \quad |\eta_{j}| < 2.5, \end{aligned} \tag{5}$$

where $\Delta R = \sqrt{\Delta\Phi^2 + \Delta\eta^2}$ is the separation in the rapidity-azimuth plane, $p_T^{\gamma,\ell,b,j}$ are the transverse momentum of photons, leptons, b-jets and jets.

Next we discuss the events selection by focusing on two cases: the $pp \to th$ (henceforth referred to as ‘Case A’) process and the $pp \to t\bar{t} \to thj$ (henceforth referred to as ‘Case B’) process, respectively. The main difference is whether there is a light jet in the final state. However, it should be mentioned that the final signals for Case B could also be considered as a source of Case A if the light quark is missed by the detector. Thus we combine these two cases when we consider the above signal events. Firstly, let us focus on the final signal for the Case A where only the events including at least two photons, exactly one b-tagged jet and one charged lepton are considered.

In Fig. 2, we plot some differential distributions for signals and SM backgrounds at the 14 TeV LHC, such as the transverse momentum distributions of the two photons, the invariant mass distributions of the two photons, $M_{\gamma_1\gamma_2}$, the transverse mass distribution for the $b\ell\not{E}_T$ systems, and the pseudorapidity of the higgs boson η^h. Here the top quark transverse cluster mass is defined as

$$M_T^2 \equiv (\sqrt{(p_\ell + p_b)^2 + |\vec{p}_{T,\ell} + \vec{p}_{T,b}|^2} + |\vec{\not{p}}_T|)^2 - |\vec{p}_{T,\ell} + \vec{p}_{T,b} + \vec{\not{p}}_T|^2, \tag{6}$$

where $\vec{p}_{T,\ell}$ and $\vec{p}_{T,b}$ are the transverse momentums of the charged leptons and b-quark, respectively, and $\vec{\not{p}}_T$ is the missing transverse momentum determined by the negative sum of visible momenta in the transverse direction.

One can see that the two photons in the signal and the resonant backgrounds have the harder p_T spectrum than those in the non-resonant backgrounds. Furthermore, the signal and the resonant backgrounds have the diphoton invariant-mass peak at m_h. Since the lepton and b-jet are assumed to originate from the leptonically decaying top quark, the cut on the transverse mass of the top candidate is needed. Besides, the Higgs boson from the $ug \to th$ process concentrates in the forwards and backwards regions because the partonic center-of-mass frame is highly boosted along the direction of the up quark. On the contrary, the main contribution of top pair production comes from gluon initial-states, which are symmetric and have small boost effect.

According to the above analysis, we can impose a further set of cuts for the Case A.

- Cut 1: There are exactly one b-jet and only one isolated lepton with positive charge.
- Cut 2: The leading (sub-leading) photons with $p_T > 60$ (30) GeV and $\Delta R_{\gamma_1,\gamma_2} < 2.0$.
- Cut 3: $|M_{\gamma_1\gamma_2} - m_h| < 5$ GeV.
- Cut 4: 100 GeV $< M_T^{b\ell} <$ 180 GeV.
- Cut 5: $|\eta_h| > 1.0$.

However, these distributions will be slightly different if we focus on the signal for the Case B, because there is a light jet which coming from one top decay $t \to hq \to \gamma\gamma q$ or one anti-top quark decay $\bar{t} \to h\bar{q} \to \gamma\gamma\bar{q}$. Thus the invariant mass distribution of the diphoton and leading light jet $M_{\gamma\gamma j}$ also has a peak around the top quark mass in the signal. In Fig. 3, we plot some distributions for the Case B. It should be noted that other distributions are similar to the previous

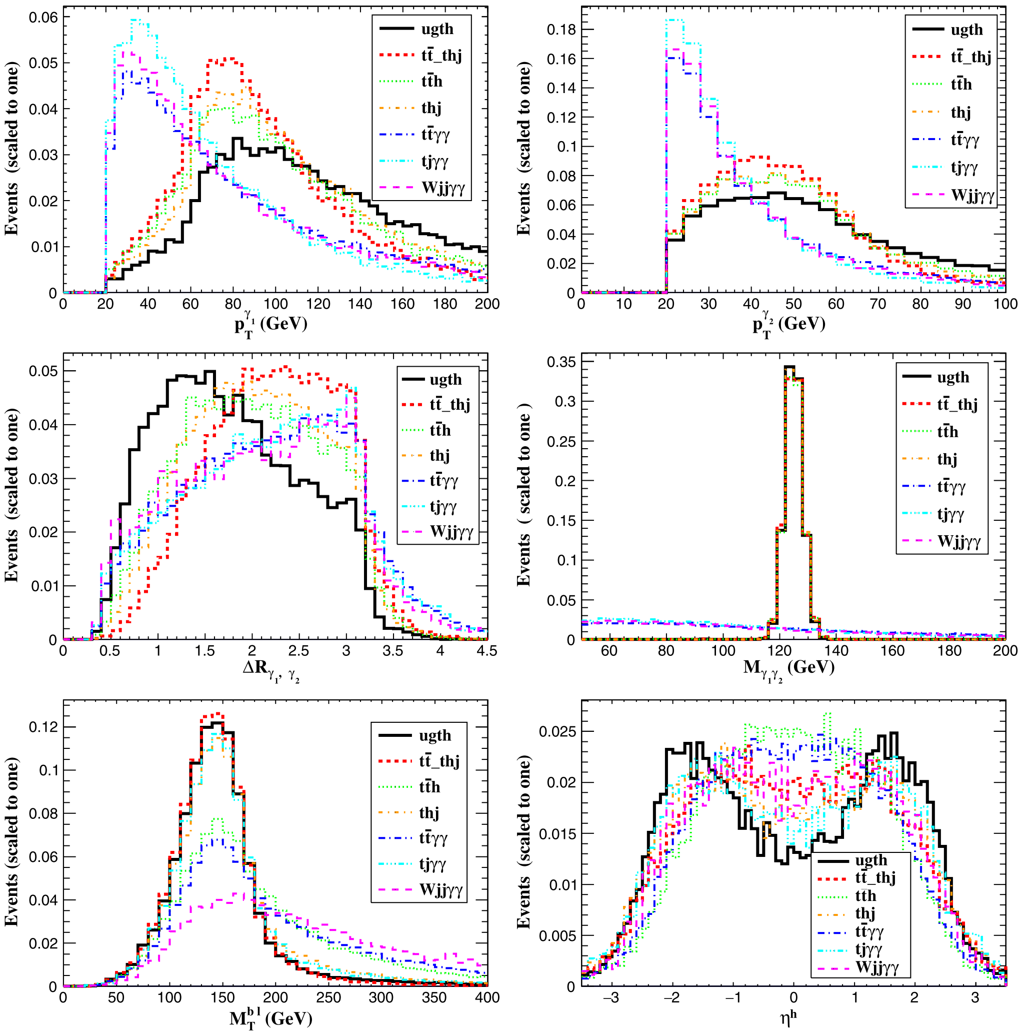

Fig. 2. Normalised distributions for the signals and SM backgrounds for the Case A. (For interpretation of the colors in the figure(s), the reader is referred to the web version of this article.)

case, such as the transverse momentum distributions of the two photons, the invariant mass distributions of the two photons and the transverse mass distribution for the $b\ell \not{E}_T$ systems. Thus the following cuts can be imposed to further remove the backgrounds if we focus on the final signals for the Case B.

- Cut 1: There are at least two jets and exactly one b-tagged jet among two, and only events with one isolated lepton are considered.
- Cut 2: There at least two photons with $p_T > 60$ GeV for leading photon and $p_T > 30$ GeV for the subleading one, and $\Delta R_{\gamma_1\gamma_2,j} < 1.5$.
- Cut 3: $|M_{\gamma_1\gamma_2} - m_h| < 5$ GeV.
- Cut 4: 100 GeV $< M_T^{b\ell} <$ 180 GeV.

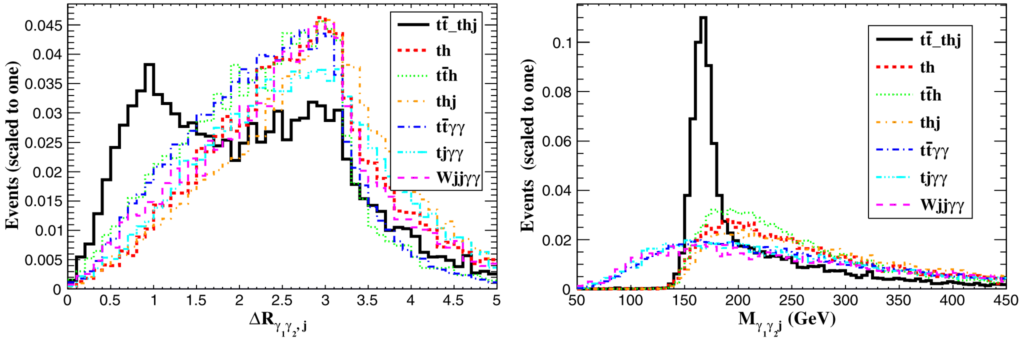

Fig. 3. Normalised distributions for the signals and SM backgrounds for the Case B.

Table 1
For the Case A, the cut flow of the cross sections (in $\times 10^{-3}$ fb) for the signals and SM backgrounds at the HL-LHC with $\kappa_{tuh} = 0.04$.

Cuts	Signal		Backgrounds					
	$ug \to th$	$t\bar{t} \to thj$	$t\bar{t}h$	thj	$t\bar{t}\gamma\gamma$	$tj\gamma\gamma$	$W^{\pm}\gamma\gamma jj$	total
Basic cuts	44	118	67	9	435	823	953	2285
Cut 1	40	54	14.8	4.5	96	396	468	979
Cut 2	17	11	4.4	1.3	11.8	35.8	55.3	109
Cut 3	15.6	10.2	4.0	1.24	0.5	1.4	2.3	9.5
Cut 4	9.8	0.67	1.7	0.8	0.1	0.7	0.9	4.2
Cut 5	6.4	3.0	0.68	0.45	0.05	0.43	0.21	1.8

- Cut 5: 150 GeV $< M_{\gamma_1\gamma_2 j} <$ 190 GeV.

The effects of the suitable cuts on the signal and SM background processes are illustrated in Tables 1-2. One can see that, at the end of the cut flow, the total SM backgrounds are only about 0.002 fb for two cases, and there are only about 6 events with the integrated luminosity of 3000 fb^{-1}. Besides, the $t\bar{t}h$ process can generate dominant contributions for the SM background. For the signals in Case A, the cross section for the $ug \to th$ process is about twice that of the $pp \to t\bar{t} \to thj$ process. For the case B, the final cross section for the $pp \to t\bar{t} \to thj$ process is about 0.01 fb, and there will be more signal events than those for Case A with the same coupling parameter κ_{tqh}. Furthermore, the final cross sections for the $pp \to th$ process are very small, i.e., 0.72×10^{-3} fb for $\kappa_{tuh} = 0.04$ and 0.15×10^{-3} fb for $\kappa_{tch} = 0.04$. Thus, we can safely neglected these contributions when we evaluate the constraints on the tch coupling for the Case B.

2.2. *Exclusion significance*

To estimate the exclusion significance for the small number of events, $Z_{\rm excl}$, we use the following expression [46]:

$$Z_{\rm excl} = \sqrt{2\left[s - b\ln\left(\frac{b+s+x}{2b}\right) - \frac{1}{\delta^2}\ln\left(\frac{b-s+x}{2b}\right)\right] - (b+s-x)\left(1+\frac{1}{\delta^2 b}\right)}, \quad (7)$$

Table 2
For the Case B, the cut flow of the cross sections (in $\times 10^{-3}$ fb) for the signals and SM backgrounds at the HL-LHC with $\kappa_{tuh} = 0.04$ or $\kappa_{tch} = 0.04$ (in the blanket) in the signal, while fixing the other to zero.

Cuts	Signal		Backgrounds					
	$t\bar{t} \to thj$	$pp \to th$	$t\bar{t}h$	thj	$t\bar{t}\gamma\gamma$	$tj\gamma\gamma$	$W^{\pm}\gamma\gamma jj$	total
Basic cuts	118	49 (10)	67	9	435	818	936	2264
Cut 1	109	45 (9)	30	7	189	642	838	1705
Cut 2	20	2.1 (0.44)	3.7	0.52	12.3	25	40	82
Cut 3	18.3	1.9 (0.4)	3.3	0.47	0.56	1.0	2.0	7.3
Cut 4	12.4	1.2 (0.3)	1.6	0.3	0.2	0.7	0.6	3.5
Cut 5	11.2	0.72 (0.15)	0.91	0.17	0.13	0.43	0.43	2.1

Table 3
The upper limits on BR($t \to qh$) at 95% CL obtained at the HL-LHC. We consider systematic errors of 0% and 20% on the SM background events. The numbers in the blanket denote the values only considering the $ug \to th$ process in Case A, and only considering the $pp \to t\bar{t} \to thj + \bar{t}hj$ process in Case B.

Upper limits	Case A		Case B	
	$\delta = 0\%$	$\delta = 20\%$	$\delta = 0\%$	$\delta = 20\%$
BR($t \to uh$)	$1.6\ (2.3) \times 10^{-4}$	$1.7\ (2.4) \times 10^{-4}$	$1.3\ (1.4) \times 10^{-4}$	$1.4\ (1.5) \times 10^{-4}$
BR($t \to ch$)	\	\	1.4×10^{-4}	1.5×10^{-4}

with $x = \sqrt{(s+b)^2 - 4\delta^2 sb^2/(1+\delta^2 b)}$. Here, the values of s and b are the total signal and SM background events, respectively. δ is the percentage systematic error on the SM background estimate. In this work we choose two cases: $\delta = 0\%, 20\%$ for HL-LHC. In the limit of $\delta \to 0$, the above expression can be simplified as $Z_{\rm excl} = \sqrt{2[s - b\ln(1+s/b)]}$. We define the regions with $Z_{\rm excl} \leq 1.645$ as those that can be excluded at 95% CL [46].

In Table 3, we list the exclusion limits at 95% CL at the future HL-LHC with the aforementioned two systematic error cases of $\delta = 0\%$ and $\delta = 20\%$. Note that the branching ratio of $t \to qh$ is approximately given by $Br(t \to qh) \simeq 0.58\kappa_{tqh}^2$ [31], thus these limits can be translated to the upper limits to the corresponding branching ratios. One can see that, the sensitivity to the $Br(t \to qh)$ are at the 10^{-4} level for both cases, i.e., even we only consider the signal from the $ug \to th$ process in Case A, the 95% CL limits on the BR($t \to uh$)'s have been found to be 2.4×10^{-4} with 20% systematic uncertainty, and the corresponding upper limit on the coupling is $\kappa_{tuh} < 0.02$. The benefit of this process is that it has the large charged ratio for lepton, which can be used to determine that the signal comes from the up initiated production channel. Due to the small events number of the SM background, the effect of systematic error is also small. For comparison, the recent 95% upper limits on BR($t \to qh$) obtained at the HL-LHC with an integrated luminosity of 3 ab^{-1} by the ATLAS Collaboration [47,48] are also presented, which are obtained via the decay mode $t \to qh(\to b\bar{b})$ and $t \to ch(\to \gamma\gamma)$, respectively. For example, an expected upper limit of BR($t \to ch$) $< 1.5 \times 10^{-4}$ at 95% CL is obtained via the decays $t \to ch(\to \gamma\gamma)$ channel [48]. Thus our estimate is in a good agreement with the dedicated study performed by the ATLAS collaboration. In general, such limits are one order of magnitude better than the most recent direct limits reported by the ATLAS Collaboration at the 13 TeV.

Next, let us to review competing limits from other authors at the HL-LHC. For instance, the author of Ref. [49] has studied the top-Higgs FCNC couplings via the $h \to WW^*$ decay channels at the HL-LHC and the upper limits of $Br(t \to uh) < 0.07\%$ and $Br(t \to ch) < 0.14\%$ were obtained. Very recently, the authors of Ref. [50] have investigated the prospect for $t \to ch$ decay in top quark pair production in the context of the 2-Higgs Doublet Model (2HDM), and find that the 95% CL upper limits on BR$(t \to ch)$ was found to be 1.17×10^{-3} at the HL-LHC.

3. Conclusion

In this work, we have studied the FCNH interactions of top quark, i.e., tqh ($q = u, c$), at the HL-LHC by performing a full simulation for two processes: $pp \to t\bar{t} \to thj$ and $pp \to th$ with the $h \to \gamma\gamma$ decay channel. If we take the percentage systematic error on the SM background estimate as 20% at the 14 TeV LHC with 3000 fb^{-1} integrated luminosity, the branching ratio $Br(t \to uh)$ ($Br(t \to ch)$) can be probed to 1.4 (1.5) $\times 10^{-4}$ at the 95% Confidence Level (CL) by focusing on the former process, while if we only consider the signal coming from the $pp \to th$ process, the upper limit on the branching ratio of about $Br(t \to uh) = 2.4 \times 10^{-4}$ at the 95% CL is obtained. Altogether, these limits are one order of magnitude better than the current experimental results obtained from LHC runs at 13 TeV. Thus we expect to provide the complementary information for detecting such anomalous couplings at the future HL-LHC.

CRediT authorship contribution statement

Jie-Fen Shen: Conceptualization, Methodology, Software, Writing - review & editing. **Yan-Ju Zhang:** Data curation, Writing - original draft.

Declaration of competing interest

The authors declare that they have no known competing financial interests or personal relationships that could have appeared to influence the work reported in this paper.

Acknowledgements

We would like thank Y.-B Liu for useful discussion. This work is supported by the Foundation of Henan Educational Committee (Grant no. 2015GGJS-059).

References

[1] G. Aad, et al., ATLAS Collaboration, Phys. Lett. B 716 (2012) 1.
[2] V. Khachatryan, et al., CMS Collaboration, Phys. Lett. B 716 (2012) 30.
[3] J.A. Aguilar-Saavedra, Acta Phys. Pol. B 35 (2004) 2695.
[4] J.A. Aguilar-Saavedra, Nucl. Phys. B 821 (2009) 215.
[5] H.J. He, C.P. Yuan, Phys. Rev. Lett. 83 (1999) 28.
[6] C. Balazs, H.J. He, C.P. Yuan, Phys. Rev. D 60 (1999) 114001.
[7] J.L. Diaz-Cruz, H.J. He, C.P. Yuan, Phys. Lett. B 530 (2002) 179.
[8] H.J. He, S. Kanemura, C.P. Yuan, Phys. Rev. Lett. 89 (2002) 101803.
[9] J. Cao, C. Han, L. Wu, J.M. Yang, M. Zhang, Eur. Phys. J. C 74 (2014) 3058.
[10] T.J. Gao, T.F. Feng, F. Sun, H.B. Zhang, S.M. Zhao, Chin. Phys. C 39 (2015) 073101.
[11] C. Kao, H.Y. Cheng, W.S. Hou, J. Sayre, Phys. Lett. B 716 (2012) 225.
[12] T. Han, R. Ruiz, Phys. Rev. D 89 (2014) 074045.
[13] G. Abbas, A. Celis, X.Q. Li, J. Lu, A. Pich, J. High Energy Phys. 1506 (2015) 005.
[14] F.J. Botella, G.C. Branco, M. Nebot, M.N. Rebelo, Eur. Phys. J. C 76 (2016) 161.
[15] M.A. Arroyo-Ureña, J.L. Diaz-Cruz, E. Díaz, J.A. Orduz-Ducuara, Chin. Phys. C 40 (2016) 123103.
[16] H.J. He, T.M.P. Tait, C.P. Yuan, Phys. Rev. D 62 (2000) 011702.
[17] H.J. He, C.T. Hill, T.M.P. Tait, Phys. Rev. D 65 (2002) 055006.

[18] B. Yang, N. Liu, J. Han, Phys. Rev. D 89 (2014) 034020.
[19] X.F. Wang, C. Du, H.J. He, Phys. Lett. B 723 (2013) 314.
[20] M. Badziak, K. Harigaya, Phys. Rev. Lett. 120 (2018) 211803.
[21] T.M.P. Tait, C.-P. Yuan, Phys. Rev. D 63 (2000) 014018.
[22] J.A. Aguilar-Saavedra, G.C. Branco, Phys. Lett. B 495 (2000) 347.
[23] Q.H. Cao, J. Wudka, C.-P. Yuan, Phys. Lett. B 658 (2007) 50.
[24] M. Aaboud, et al., ATLAS Collaboration, J. High Energy Phys. 1710 (2017) 129.
[25] M. Aaboud, et al., ATLAS Collaboration, Phys. Rev. D 98 (2018) 032002.
[26] M. Aaboud, et al., ATLAS Collaboration, J. High Energy Phys. 1905 (2019) 123.
[27] A.M. Sirunyan, et al., CMS Collaboration, J. High Energy Phys. 1806 (2018) 102.
[28] X. Chen, L. Xia, Phys. Rev. D 93 (2016) 113010.
[29] S. Khatibi, M.M. Najafabadi, Phys. Rev. D 89 (2014) 054011.
[30] D. Atwood, S.K. Gupta, A. Soni, J. High Energy Phys. 1410 (2014) 057.
[31] Y.B. Liu, Z.J. Xiao, Phys. Lett. B 763 (2016) 458.
[32] A. Greljo, J.F. Kamenik, J. Kopp, J. High Energy Phys. 1407 (2014) 046.
[33] Y.B. Liu, Z.J. Xiao, Phys. Rev. D 94 (2016) 054018.
[34] L. Wu, J. High Energy Phys. 1502 (2015) 061.
[35] J. Alwall, R. Frederix, S. Frixione, V. Hirschi, F. Maltoni, O. Mattelaer, H.-S. Shao, T. Stelzer, P. Torrielli, M. Zaro, J. High Energy Phys. 1407 (2014) 079.
[36] R.D. Ball, et al., NNPDF Collaboration, J. High Energy Phys. 1504 (2015) 040.
[37] M. Tanabashi, et al., Particle Data Group, Phys. Rev. D 98 (2018) 030001.
[38] Y-B. Liu, S. Moretti, Phys. Rev. D 101 (2020) 075029.
[39] T. Sjöstrand, S. Ask, J.R. Christiansen, et al., Comput. Phys. Commun. 191 (2015) 159.
[40] J. de Favereau, et al., DELPHES 3 Collaboration, J. High Energy Phys. 1402 (2014) 057.
[41] E. Conte, B. Fuks, G. Serret, Comput. Phys. Commun. 184 (2013) 222.
[42] M. Cacciari, G.P. Salam, G. Soyez, Eur. Phys. J. C 72 (2012) 1896.
[43] Y. Wang, F.P. Huang, C.S. Li, B.H. Li, D.Y. Shao, J. Wang, Phys. Rev. D 86 (2012) 094014.
[44] Y. Zhang, W.G. Ma, R.Y. Zhang, C. Chen, L. Guo, Phys. Lett. B 738 (2014) 1.
[45] M. Czakon, P. Fiedler, A. Mitov, Phys. Rev. Lett. 110 (2013) 252004.
[46] G. Cowan, K. Cranmer, E. Gross, O. Vitells, Eur. Phys. J. C 71 (2011) 1554;
G. Cowan, K. Cranmer, E. Gross, O. Vitells, Eur. Phys. J. C 73 (2013) 2501 (Erratum).
[47] ATLAS Collaboration, ATL-PHYS-PUB-2016-019.
[48] ATLAS Collaboration, ATL-PHYS-PUB-2013-012.
[49] Y.B. Liu, S. Moretti, Chin. Phys. C 43 (2019) 013102.
[50] R. Jain, C. Kao, Phys. Rev. D 99 (2019) 055036.